Article ID: 1003－6326(2003)06－1354－06

Numerical simulation of influence of viscous adhesive stress on viscous pressure bulging process of hemispherical sphere①

LIU Jian-guang(刘建光), WANG Zhong-jin(王忠金), WANG Zhong-ren(王仲仁)
(School of Materials Science and Engineering, Harbin Institute of Technology, Harbin 150001, China)

Abstract: The mechanical model of viscous pressure bulging process is presented. The viscous pressure bulging process of hemispherical sphere is analyzed by the numerical simulation and experiments. The research results show that the viscosity of viscous medium significantly affected the thickness distribution, strain distribution and shape of hemispherical sphere, which provides analytic basis for selecting reasonably viscous medium and designing process of viscous pressure forming.

Key words: viscous pressure forming(VPF); hemispherical sphere; bulging; numerical simulation; viscous adhesive stress

CLC number: TG 316 **Document code:** A

1 INTRODUCTION

Viscous pressure forming(VPF) is a new developed technology for sheet metal flexible forming, which uses a kind of semi-solid, flowable and viscous medium as pressure-carrying medium[1-5]. Sheet metal is affected not only by normal pressure of viscous medium but also by tangent adhesive stress of viscous medium in VPF process. The action of viscous medium on sheet metal improves sheet metal formability. It can postpone local necking in the sheet metal and can make the thickness distribute uniformly[6-9].

The viscosity of viscous medium is one of the most important factors that affect the sheet metal deformation. Because of only less research on the influence of viscous medium on deformation of sheet metal, there are not enough academic base for selecting the viscous medium and designing VPF process. In this paper, the tangent adhesive stress of viscous medium is introduced into the updated Lagrange finite element formulation based on Mindlin degenerated shell element. An elasto-plastic FEA code is developed to analyze the viscous pressure bulging process of sheet metal. The influence of viscosity of viscous medium on thickness distribution, strain distribution and shape of hemispherical sphere are investigated, which provides analytic basis for selecting reasonably viscous medium of VPF and designing VPF process.

2 MECHANICAL MODEL OF VISCOUS PRESSURE BULGING

Compared with hydro-bulging process and rigid punch bulging process, viscous pressure bulging process has some unique characteristics. Firstly, the pressure distribution of viscous medium during viscous pressure bulging process is non-uniform and is different from that of hydro-bulging process(in later case it is uniform). Secondly, sheet metal is applied by the tangent adhesive stress of viscous medium during the whole forming process. The value of tangent adhesive stress is affected by the viscous medium pressure, viscosity and forming time. With the increase of load, the viscous medium pressure and the tangent adhesive stress become higher[10]. In addition, the tangent adhesive stress is also the function of forming time. To express the relationship between the tangent adhesive stress and the normal pressure of viscous medium, the coefficient of tangent adhesive stress C_v is defined as the value of the tangent adhesive stress yielded by unit normal pressure of viscous medium. The tangent adhesive stress coefficient is related to the viscosity of viscous medium, forming time and the viscous medium pressure and varies during the viscous pressure bulging process. This phenomenon is different from the friction between sheet metal and rigid punch in the rigid punch forming process.

The mechanical model of viscous pressure bulging is shown in Fig. 1(p denotes the normal pressure of viscous medium, τ is the tangent adhesive stress). Assuming that the tangent adhesive stress be in proportion to normal pressure of viscous medium, the tangent adhesive stress can be calculated by Eqn. (1)

① **Foundation item:** Project(50275035) supported by the National Natural Science Foundation of China
Received date: 2003－01－08; **Accepted date:** 2003－04－14
Correspondence: LIU Jian-guang; Tel: +86-451-86413365; E-mail: liujg@hit.edu.cn

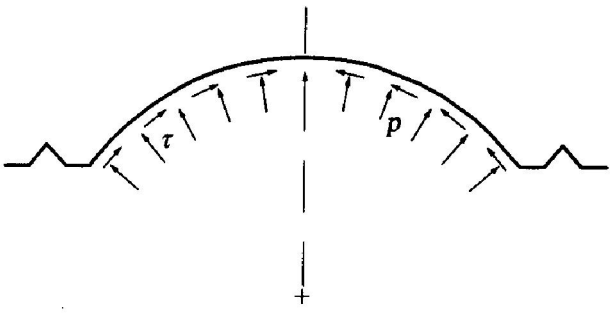

Fig. 1 Mechanical model of viscous pressure bulging process

$$\tau = C_v(p, \eta, t)p(x, y, z, t) \tag{1}$$

where C_v denotes the tangent adhesive stress coefficient, η is the viscosity of viscous medium, t is forming time and x, y, z denote the nodal coordinate.

3 FINITE ELEMENT MODEL

3.1 Mindlin thick-shell element model[11]

A 4-node degenerated shell element based on Mindlin-Reissner theory is employed for the finite element numerical simulation, as shown in Fig. 2. $X_1X_2X_3$ is the global Cartesian coordinate system, $x'y'z'$ is the node coordinate system, $\xi\eta\zeta$ is the natural coordinate system, and $x_1x_2x_3$ is the local coordinate system. The displacement of an arbitrary point in the element can be expressed by shape function $N_i(\xi, \eta)$ and the displacement $[u_i, v_i, w_i]$ of the mid-surface nodes.

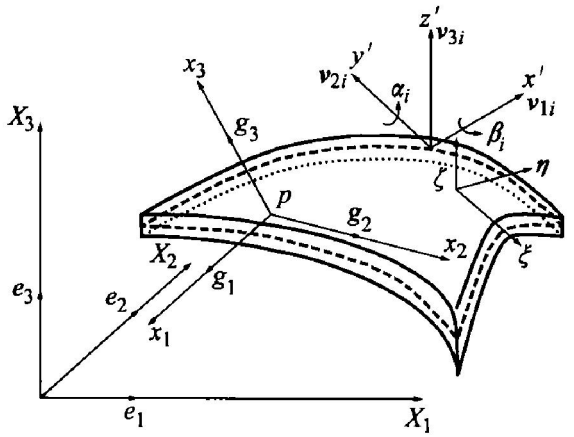

Fig. 2 4-node Mindlin thick-shell element

$$\begin{Bmatrix} u \\ v \\ w \end{Bmatrix} = \sum_{i=1}^{4} N_i(\xi, \eta) \cdot \left(\begin{Bmatrix} u_i \\ v_i \\ w_i \end{Bmatrix} + \frac{\zeta t_i}{2}[V_{1i} - V_{2i}] \begin{Bmatrix} \alpha_i \\ \beta_i \end{Bmatrix} \right) \tag{2}$$

where t_i is the thickness of element; α_i and β_i mean the normal rotation of the mid-surface; V_{1i} and V_{2i} are the unit vectors of node coordinate system.

3.2 Constitutive equation

With constitute relation of the Jaumann rate of Cauchy stress and the von Mises yield criterion, the constitute equation under local coordinate can be expressed as[12]

$$\sigma_{ij}^{\nabla} = D_{ijkl}^{ep}\dot{\varepsilon}_{kl} \tag{3}$$

where σ_{ij}^{∇} denotes the Jaumann rate of Cauchy stress under local coordinate x_i.

D_{ijkl}^{ep} represents the elasto-plastic stress-strain matrix, which is

$$D_{ijkl}^{ep} = \frac{E}{1+\mu}\left\{ \left[\frac{1}{2}(\delta_{ik}\delta_{jl} + \delta_{il}\delta_{jk}) + \frac{\mu}{1-2\mu}\delta_{ij}\delta_{kl} \right] - \frac{3}{2}\frac{\sigma'_{ij}\sigma'_{kl}}{\bar{\sigma}^2\left[1 + \frac{2}{3}H'(1+\mu)/E\right]} \right\} \tag{4}$$

where δ_{ij} is Kronecker delta, μ is the Poisson ratio, E is the elastic modulus, H' is the slope of the stress—plastic strain curve, $\bar{\sigma}$ is the effective stress, and σ'_{ij} is the deviatoric stress tensor.

3.3 Element equilibrium equation

The virtual work-rate principle of finite deformation with updated Lagrange formulation is employed[13]:

$$\int_V \dot{t}_{ij}\delta\left[\frac{\partial v_j}{\partial X_1}\right] dV = \int_V \dot{f}^b \delta v_i dA + \int_{A_T} \dot{f}^S \delta v_i dA \tag{5}$$

where $\dot{t}_{ij}$ denotes the first Piola-Kirchhoff stress rate sensor; V and A_T are the volume and surface area of element respectively; $\dot{f}^b$ and $\dot{f}^S$ are the applied external volume and surface force, respectively; $\frac{\partial v_j}{\partial X_1}$ is the velocity gradient.

When the tangent adhesive stress $\dot{\tau}_i$ is introduced into above formulation under local coordinate system and the volume force is ignored, there is

$$\int_V \dot{t}_{ij}\delta\left[\frac{\partial v_j}{\partial X_1}\right] dV = \int_{A_T} d\dot{p}_1 \delta v_i dA + \int_{A_T} d\dot{\tau}_i \delta v_i dA \tag{6}$$

where $\dot{p}$ and $\dot{\tau}_i$ are the normal pressure rate and the tangent adhesive stress rate, respectively.

The incompressibility of plastic deformation volume is assumed, then the relation between the Jaumann rate of Cauchy stress σ_{ij}^{∇} and the first Piola-Kirchhoff stress rate $\dot{t}_{ij}$ can be obtained

$$\dot{t}_{ij}(t) = \sigma_{ij}^{\nabla} - \sigma_{ik}\dot{\varepsilon}_{kj} - \sigma_{kj}\dot{\varepsilon}_{ki} + \sigma_{ik}v_{j,k} \tag{7}$$

Now substituting Eqns. (3) and (7) into Eqn. (6), yields

$$\int_V \left[(\bar{D}_{ijkl}^{ep} - F_{ijkl})\dot{\varepsilon}_{kl}\delta\dot{\varepsilon}_{ij} + \sigma_{ik}v_{j,k}\delta v_{j,i} \right] dV = \int_{A_T} \dot{p}_i \delta v_i dA + \int_{A_T} \dot{\tau}_i \delta v_i dA \tag{8}$$

The element equilibrium equation is represented in matrix form:

$$[K]\{d\}^e = \{\dot{F}\}^e \tag{9}$$

where

$$\{\dot{F}\} = \int_{A_T} N^T \theta\dot{p}\, dA + \int_{A_T} N^T \theta\dot{\tau}\, dA \quad (10)$$

$$[K] = \int_V \{B^T(\overline{D}^{ep} - F)B + B_V^T Q B_V\} dV \quad (11)$$

According to the above theory, a three dimensional elasto-plastic FEA code was developed for analyzing the viscous pressure bulging process.

4 VERIFICATION OF NUMERICAL SIMULATION PROCEDURE

In order to validate numerical simulation method presented in this paper, numerical simulation and experiments are conducted respectively for hydro-bulging process and viscous pressure bulging process of circular sheet.

4.1 Hydro-bulging of hemispherical sphere

The experimental material is LY12, its initial thickness is 0.89 mm and the property parameters are listed in Table 1.

Table 1 Property parameters of experimental material LY12

State	E/GPa	μ	n	σ_s/MPa
Anneal	71	0.3	0.269	110

The shape curves of sections along radius direction of sheet specimens obtained by numerical simulation and experiments are shown in Fig. 3. The numerical simulation results show good agreement with that of commercial FE code DYNAFORM and experimental ones.

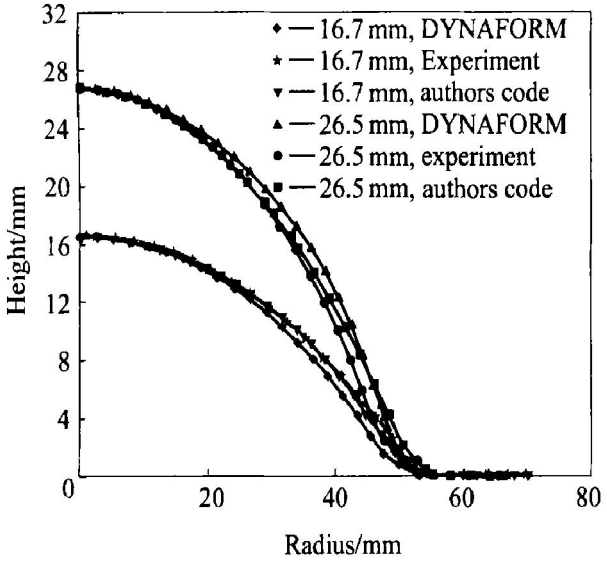

Fig. 3 Shape curves of sections along radius direction of sheet specimens obtained by numerical simulations and hydro-bulging experiments

4.2 Viscous pressure bulging of hemispherical sphere

The shape curves of sections along radius direction of sheet specimens obtained by the numerical simulation and experiment are shown in Fig. 4 at the same viscous pressure bulging height. The results of numerical simulation show a little difference from experimental ones. This is the reason why the pressure distribution of viscous medium near sheet metal is not accurately measured[14].

The shape curves of sections along radius direction of sheet specimens of viscous pressure bulging and hydro-bulging by numerical simulations are shown in Fig. 5. It can be seen that two curves are different. The shape of sheet specimens with viscous pressure bulging process tends to hemisphere because the pressure distribution of viscous medium is non-uniform in viscous pressure bulging process.

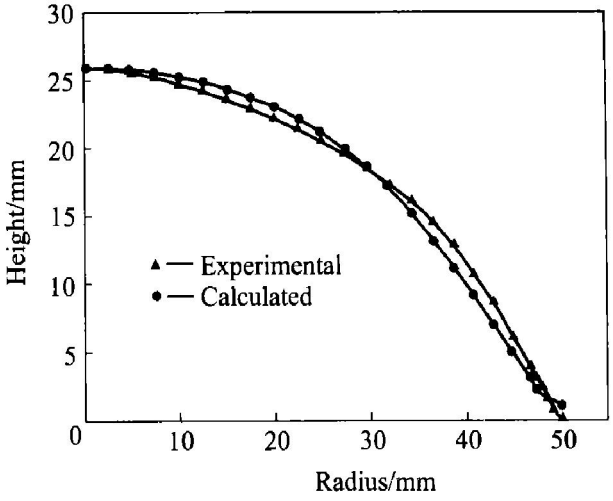

Fig. 4 Shape curves of section along radius direction of sheet specimens obtained by numerical simulation and experiment for viscous pressure bulging

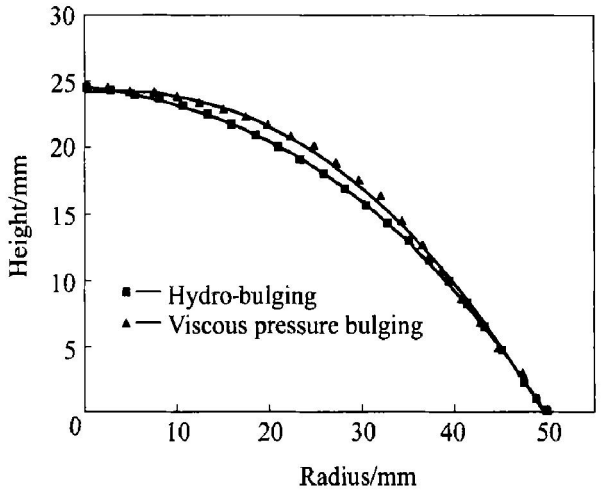

Fig. 5 Shape curves of sections along radius direction of sheet specimens calculated by numerical simulations for viscous pressure bulging and hydro-bulging

5 INFLUENCE OF TANGENT ADHESIVE STRESS ON VISCOUS PRESSURE BULGING OF HEMISPHERICAL SPHERE

In order to analyze the influence of tangent adhesive stress on viscous pressure bulging process, numerical simulation method is used to research the influence of tangent adhesive stress on thickness distribution and strain distribution of sheet metal under different values of tangent adhesive stress. Two pressure distribution modes of viscous medium are shown in Fig. 6 and can be obtained by varying the position of inject nozzle.

The property parameters of sheet metal are listed in Table 1 and its initial thickness is 0.89 mm. The diameter of die is 100 mm.

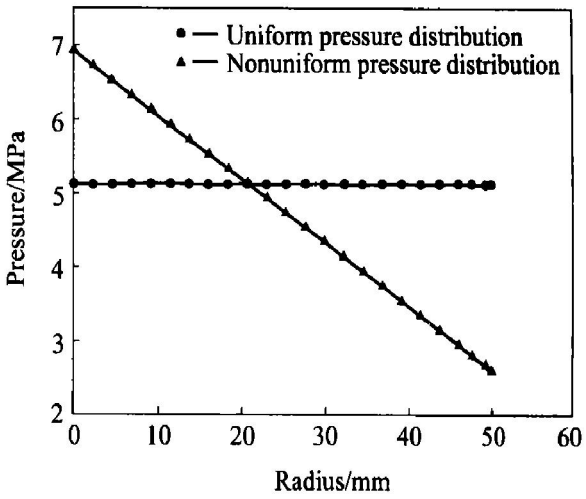

Fig. 6 Pressure distribution modes of viscous medium used for numerical simulation of viscous pressure bulging

5.1 Influence of tangent adhesive stress on meridional strain and latitudinal strain distribution

The meridional and latitudinal strain distribution curves calculated by different tangent adhesive stress coefficients and obtained by experiment are shown in Fig. 7 and Fig. 8 respectively at the same viscous pressure bulging height. With the increase of the tangent adhesive stress coefficients, the meridional strain in dome center area gradually reduces

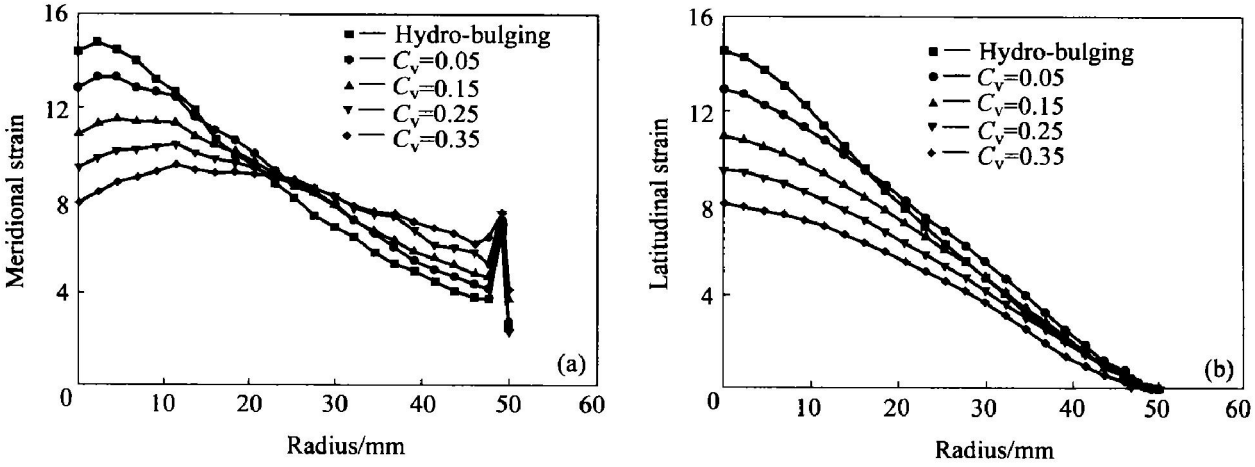

Fig. 7 Meridional and latitudinal strain distribution curves obtained by numerical simulations of viscous pressure bulging under uniform pressure mode of viscous medium
(a) —Meridional strain; (b) —Latitudinal strain

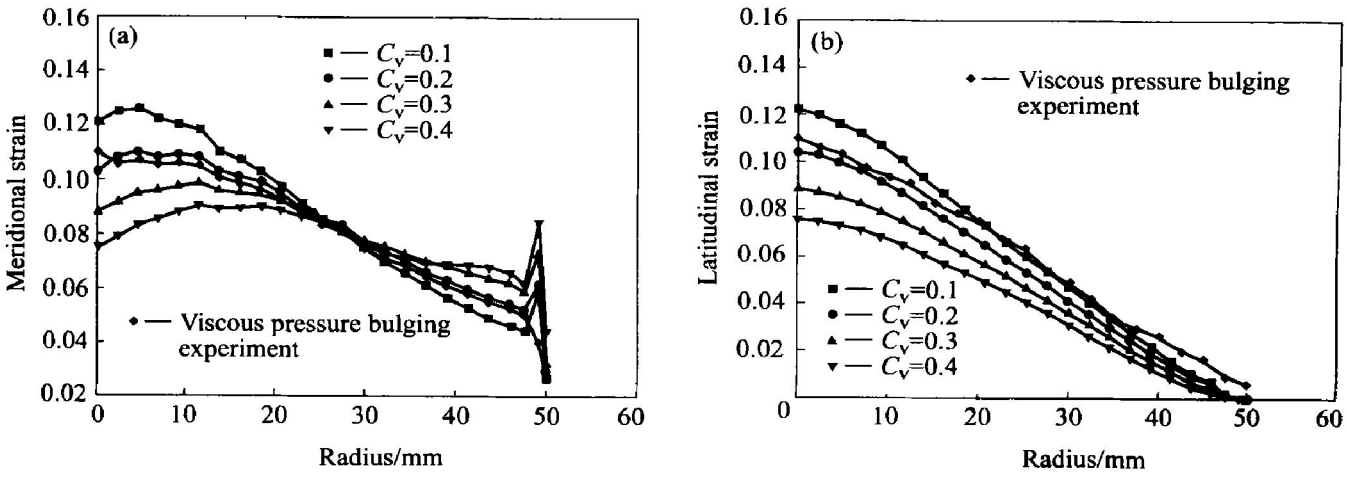

Fig. 8 Meridional and latitudinal strain distribution curves obtained by numerical simulations and experiment of viscous pressure bulging under non-uniform pressure mode of viscous medium
(a) —Meridional strain; (b) —Latitudinal strain

and the meridional strain near die entrancearea gradually increases. The tangent adhesive stress would change the meridional strain distribution of sheet specimens.

With the increase of the tangent adhesive stress coefficient in the condition of the same pressure distribution mode of viscous medium, however, the latitudinal strain gradually reduces. The reduction of the meridional strain and the latitudinal strain in dome center areas postpone the local necking of hemispherical sphere.

5.2 Influence of tangent adhesive stress on thickness distribution

The thickness distribution curves of sheet specimens calculated by different tangent adhesive stress coefficients and obtained by experiment are shown in Fig. 9 and Fig. 10 at the same viscous pressure bulging height. When the tangent adhesive stress coefficient is lower, the maximum thickness reduction of sheet specimens appears in dome center area and the thickness gradually increases from the dome center to the die entrance. The thickness distribution is similar to that of hydro-bulging process. With the increase of the tangent adhesive stress coefficient, the thickness of sheet specimen in dome center area gradually increases and then decreases in die entrance area and the thickness distribution tends to uniform. The thickness distribution is similar to that of rigid punch bulging process. In addition, it can also be seen that the thickness distribution of sheet specimens of viscous pressure bulging is obviously more uniform than that of hydro-bulging. It can be seen from Fig. 8 and Fig. 10 that the adhesive stress coefficient of viscous medium adopted by experiment is between 0.1 and 0.2, which provides analytical basis for qualitatively selecting viscous medium.

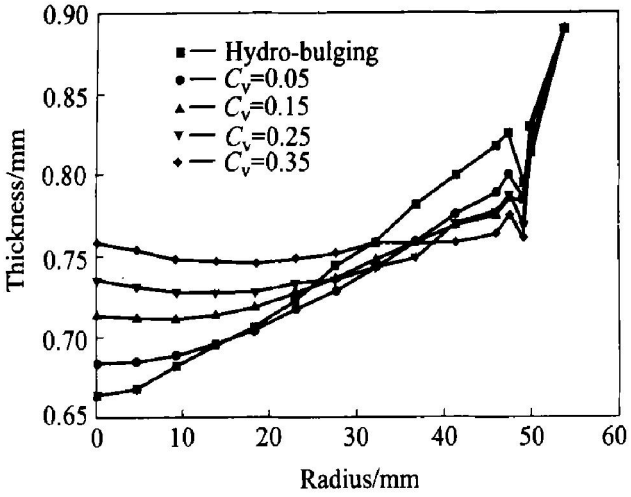

Fig. 9 Thickness distribution curves of sheet specimens obtained by numerical simulations of viscous pressure bulging under uniform pressure distribution mode

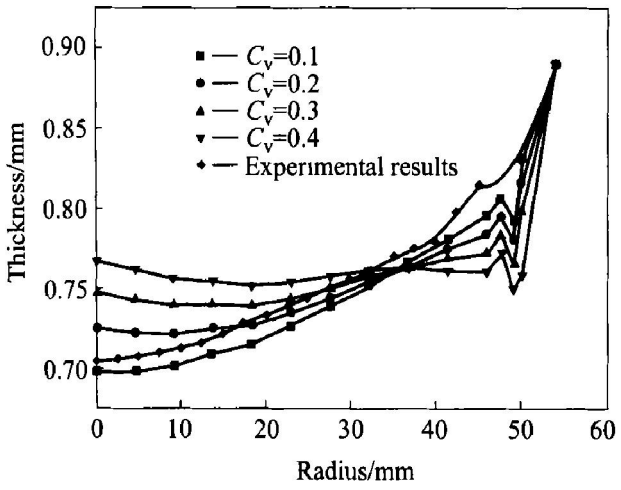

Fig. 10 Thickness distribution curves of sheet specimens obtained by numerical simulations and experiment of viscous pressure bulging under non-uniform pressure distribution mode

6 CONCLUSIONS

1) The calculated shape of sheet specimens of viscous pressure bulging is in good agreement with that of sheet specimens measured by experiments. This means that the mechanical model and the numerical simulation method for viscous pressure bulging presented in this paper is valid.

2) The shape of sheet specimens obtained by viscous pressure bulging shows obviously difference with that by hydro-bulging. Viscous pressure bulging is obviously different from hydro-bulging. The sheet specimens with different shape can be obtained through designing and controlling the pressure distribution mode of viscous medium.

3) When the tangent adhesive stress coefficient is lower, the viscous pressure bulging process is similar to hydro-bulging process and the necking occurs in dome center area. With the increase of the tangent adhesive stress, the thickness distribution of sheet specimens tends to uniform. When the tangent adhesive stress exceeds the critical coefficients of 0.35 – 0.45, the thickness distribution of sheet specimens becomes more non-uniform. The numerical simulation predicting method provides analytical basis for qualitative selecting viscous medium.

REFERENCES

[1] Liu J, Westhoff B, Ahmetogla M, et al. Application of Viscous Pressure Forming(VPF) to low volume stamping of difficult-to-forming alloys —results of preliminary FEM simulations [J]. J Mater Process Technol, 1996, 53(1): 49 – 58.

[2] Roades M L, Roades L J. Method and Apparatus for Die Forming Sheet Materials [P]. US 5085068, 1992-02-04.

[3] Ahmetoglu M A, Linzel G L, Altan T. Improvement of part quality in stamping by controlling blank-holder force

and pressure[J]. J Mater Process Technol, 1992, 33(1): 195-214.

[4] Liu J, Ahmetoglu M, Altan T. Evaluation of sheet metal formability, Viscous Pressure Forming (VPF) dome test [J]. Journal of Material Processing Technology, 2000, 98: 1-6.

[5] WANG Zhong-jin, WANG Zhong-ren, YANG Hai-feng. Experimental investigation for viscous medium drawing of sheet metal under the condition of non-uniform blank holder force[J]. Journal of Plasticity Engineering, 1999, 6(2): 50-52. (in Chinese)

[6] Shulkin Leonid B, Posteraro Ronald A, Ahmetoglu Mustafa A, et al. Blank Holder Force(BHF) control in Viscous Pressure Forming(VPF) of sheet metal[J]. J Mater Process Technol, 2000, 98: 7-16.

[7] WANG Zhong-jin, WANG Zhong-ren. Analysis of strain rate variations during viscous pressure bulging of sheet metal[J]. Journal of Plasticity Engineering, 1999, 6(3): 46-48. (in Chinese)

[8] WANG Zhong-jin, WANG Xin-yun, WANG Zhong-ren. The experimental investigation of viscous pressure-forming the ladder part[J]. Forging and Stamping Technology, 2001, 26(4): 31-33. (in Chinese)

[9] WANG Zhong-jin, WANG Xin-yun, WANG Zhong-ren. Effect of blank holder pressure on viscous pressure forming aluminum alloy ladder parts[J]. Trans Nonferrous Met Soc China, 2002, 12(1): 109-114.

[10] MA De-zhu, HE Pin-sheng. Structure and Property of Polymer[M]. Beijing: Science press, 2000. 11.

[11] Ahmad S, Irons B M, Zienkiewkcz O C, et al. Analysis of thick and thin shell structure by curved finite element [J]. Int J Num Maths, 1970, 2(4): 509-522.

[12] Kawka M, Makinouchi A. Plastic anisotropy in FEM analysis using degenerated solid element[J]. Journal of Material Processing Technology, 1996, 60: 239-242.

[13] McMeeking R M, Rice J R. Finite element for problems of large elastic-plastic deformation[J]. Int J Solids Structure, 1975, 11(5): 601-616.

[14] LIU Jian-guang. Finite Element Simulation and Experiment Research on Viscous Pressure Hemisphere Bulging Process of Sheet Metal[D]. Harbin: Harbin institute of technology, 2002. 7. (in Chinese)

(Edited by YANG Bing)